BIOCHEMISTRY
including biophysical chemistry & molecular biology

Article

pubs.acs.org/biochemistry

The Human Liver Fatty Acid Binding Protein T94A Variant Alters the Structure, Stability, and Interaction with Fibrates

Gregory G. Martin,[†] Avery L. McIntosh,[†] Huan Huang,[†] Shipra Gupta,[‡] Barbara P. Atshaves,[‡] Kerstin K. Landrock,[§] Danilo Landrock,[§] Ann B. Kier,[§] and Friedhelm Schroeder*[,†]

[†]Department of Physiology and Pharmacology, Texas A&M University, TVMC, College Station, Texas 77843-4466, United States
[‡]Department of Biochemistry and Molecular Biology, Michigan State University, East Lansing, Michigan 48824, United States
[§]Department of Pathobiology, Texas A&M University, TVMC, College Station, Texas 77843-4467, United States

ABSTRACT: Although the human liver fatty acid binding protein (L-FABP) T94A variant arises from the most commonly occurring single-nucleotide polymorphism in the entire FABP family, there is a complete lack of understanding regarding the role of this polymorphism in human disease. It has been hypothesized that the T94A substitution results in the complete loss of ligand binding ability and function analogous to that seen with L-FABP gene ablation. This possibility was addressed using the recombinant human wild-type (WT) T94T and T94A variant L-FABP and cultured primary human hepatocytes. Nonconservative replacement of the medium-sized, polar, uncharged T residue with a smaller, nonpolar, aliphatic A residue at position 94 of the human L-FABP significantly increased the L-FABP α-helical structure content at the expense of β-sheet content and concomitantly decreased the thermal stability. T94A did not alter the binding affinities for peroxisome proliferator-activated receptor α (PPARα) agonist ligands (phytanic acid, fenofibrate, and fenofibric acid). While T94A did not alter the impact of phytanic acid and only slightly altered that of fenofibrate on the human L-FABP secondary structure, the active metabolite fenofibric acid altered the T94A secondary structure much more than that of the WT T94T L-FABP. Finally, in cultured primary human hepatocytes, the T94A variant exhibited a significantly reduced extent of fibrate-mediated induction of PPARα-regulated proteins such as L-FABP, FATP5, and PPARα itself. Thus, while the T94A substitution did not alter the affinity of the human L-FABP for PPARα agonist ligands, it significantly altered the human L-FABP structure, stability, and conformational and functional response to fibrate.

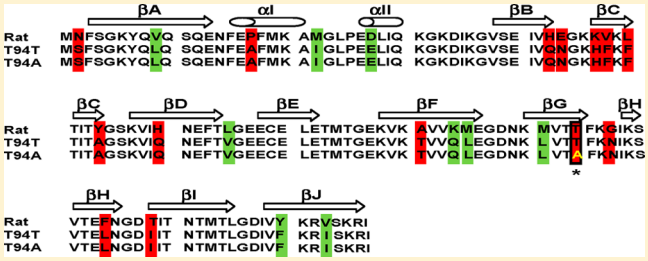

Liver fatty acid binding protein (L-FABP or FABP1) is the first member of the large FABP family to be discovered and arguably the most unique.[1−4] Unlike other family members, L-FABPs from a variety of species (e.g., rat, bovine, and human) have a much larger ligand binding cavity that accommodates two ligands instead of one.[4−14] The L-FABP has broader specificity for binding not only straight-chain LCFA but also more potent peroxisome proliferator-activated receptor α (PPARα) agonists such as the naturally occurring branched-chain LCFA phytanic acid[15−17] and less toxic xenobiotic fibrates[6,9,11,12,18,19] and phthalates.[20] An intriguing result of structural,[12,21,22] *in vitro*,[23] cultured cell,[24−27] and primary mouse hepatocyte studies[28−31] was the discovery that the L-FABP provides a signaling pathway for both natural (i.e., very long-chain polyunsaturated fatty acids) and xenobiotic (fibrates) ligands to the nucleus. In this pathway, the L-FABP binds ligands (LCFA, fatty acid synthesis inhibitors, and fibrates)[7−9,11,19,36,37] in the cytosol for cotransport into nuclei[32−35] and targets[23,25,26,28,37] bound ligands to nuclear PPARα to activate transcription of genes involved in LCFA uptake, transport, and metabolism.[24,28−31]

X-ray and nuclear magnetic resonance (NMR) demonstrated that the human liver L-FABP has an even larger binding cavity than any other mammalian L-FABP, suggesting that results from other species' L-FABPs may not necessarily be straightforwardly extrapolated to the human L-FABP.[12−14,38−42] The recent discovery of a SNP in the human L-FABP coding sequence that resulted in a single-amino acid substitution, T94A, has added further complexity to this issue.[43,44] This is especially important because the human L-FABP T94A variant is very common (26−38% minor allele frequency; 8.3 ± 1.9% homozygous; MAF for 1000 genomes in the NCBI dbSNP database; ALFRED database) and is the most prevalent polymorphism in the FABP family.[43,45−50] Further, the L-FABP T94A variant has been associated with elevated plasma triglycerides levels,[44,45] increased LDL cholesterol levels,[45,49] atherothrombotic cerebral infarction,[47] and non-alcoholic fatty liver disease (NAFLD).[49] The L-FABP ligand fenofibrate (most commonly prescribed fibrate activator of PPARα in the United States and Canada[51]) is less effective in lowering elevated plasma triglyceride levels to basal levels in L-FABP T94A variant subjects.[44] Resolving the molecular basis

Received: July 26, 2013
Revised: October 31, 2013
Published: December 3, 2013

   dx.doi.org/10.1021/bi401014k | *Biochemistry* 2013, 52, 9347−9357

for this difference is important for future therapeutic studies whereby newer fibrates might be better targeted by the L-FABP or T94A variant L-FABP to activate PPARα in the nucleus.

On the basis of the findings described above, we re-examined the literature to determine whether earlier structural studies were performed with recombinant human L-FABP-derived WT T94T L-FABP or T94A variant coding cDNAs. Fortuitously, all previously cloned human L-FABPs were derived from human WT T94T L-FABP cDNA.[52−54] Thus, all studies characterizing the ligand specificity,[9,12,40,55] structure,[13,14,38,39] and mode of ligand binding[12−14] of the human L-FABP were performed with the WT T94T L-FABP, or the phenotype of the human L-FABP was not reported.[41,42] While it has been suggested that the T94A substitution abolished binding of ligand to the human L-FABP,[56] there have been no reports actually examining the structure or ligand binding specificity of the human L-FABP T94A variant protein. To begin to resolve these issues, studies with purified recombinant human WT and T94A variant L-FABPs were initiated. As shown by CD and UV spectroscopy as well as fluorescence displacement assays, the human T94A variant L-FABP differed significantly in secondary structure, thermal stability, and structural response to fenofibric acid binding from the human WT T94T L-FABP. Finally, T94A weakened fenofibrate-mediated induction of PPARα transcriptional activity in human hepatocytes. Such dissimilarities may contribute to the impaired therapeutic response of human T94A variant L-FABP-expressing subjects to fenofibrate.[44]

EXPERIMENTAL PROCEDURES

Materials. Luria-Bertani (LB) broth and LB agar were purchased from Becton, Dickinson Co. (Sparks, MD). Fenofibrate and fenofibric acid were obtained from Santa Cruz Biotechnology (Dallas, TX). ANS (1-anilinonaphthalene-8-sulfonic acid) was purchased from Life Technologies (Grand Island, NY). Phytanic acid, ampicillin (sodium salt), isopropyl β-D-galactoside (IPTG), ammonium sulfate, protamine sulfate, dithiothreitol (DTT), and all other common laboratory chemicals were obtained from Sigma-Aldrich (St. Louis, MO). Mini-PROTEAN TGX any kD precast polyacrylamide gels and Precision Plus Protein Dual Xtra Standards were purchased from Bio-Rad (Hercules, CA). SimplyBlue SafeStain was from Invitrogen (Carlsbad, CA). All reagents and solvents were of the highest grade available.

Recombinant L-FABP Expression in *Escherichia coli*. The recombinant rat L-FABP was expressed in *E. coli* as described previously.[8,57] The cDNA for human L-FABP (NM_001443) was purchased from OriGene Technologies (Rockville, MD). The full-length human L-FABP was amplified using primers 5′-CAGCCATATGAGTTTCTCCGGCAAGTAC-3′ and 5′-GGTGCTCGAGTTAAATTCTCTTGCTGATTCTC-3′ with restriction sites *Bam*HI and *Hin*dIII, respectively, and was cloned into the pQE9-His vector (Qiagen, Valencia, CA). The cDNA purchased from OriGene was determined to be the human L-FABP T94A mutant (i.e., nucleotide 280 was guanine instead of adenine, resulting in a substitution of alanine for threonine). The mutation was established by sequencing at the Research Technology Support Facility (RTSF, Michigan State University). To obtain the T94T wild-type (WT) human L-FABP, site-directed mutagenesis was performed with primers 5′-CAATAAACTGGTGACAACTTTCAAAAACATCAAG-3′ and 5′-CTTGATGTTTTTGAAAGTTGTCACCAGTTTATTG-3′ utilizing *PfuTurbo* DNA polymerase (Agilent Technologies, Santa Clara, CA). The final WT T94T and T94A mutant constructs were transformed into *E. coli* C43 (Lucigen Corp., Middleton, WI) for protein expression.

Recombinant L-FABP Purification. The recombinant rat L-FABP was purified as described previously.[8,57] Briefly, transformed *E. coli* (expressing the WT T94T L-FABP or T94A) were streaked onto LB agar plates containing ampicillin (50 μg/mL). Plates were incubated overnight at 37 °C, and individual colonies were picked and inoculated into 100 mL of LB/ampicillin (50 μg/mL) and incubated overnight at 37 °C in a shaking incubator (250 rpm). Ten milliliters of the overnight culture were added to 1 L of LB/ampicillin (50 μg/mL) and incubated at 37 °C in a shaking incubator (250 rpm) until the optical density (OD) at 600 nm reached 0.6 absorbance unit (4−5 h for *E. coli* C43). Protein expression was induced by adding IPTG (final concentration of 1 mM) to each 1 L culture. The cultures were incubated for 12 h at 37 °C in a shaking incubator (250 rpm). Bacterial cells were harvested by centrifugation in a Beckman Avanti J-25 centrifuge (JA-14 rotor, 10000*g*, 15 min, 4 °C). Each cell pellet was resuspended in ice-cold NPND buffer [20 mM sodium phosphate (pH 7.4), 100 mM NaCl, and 1 mM dithiothreitol] containing protease inhibitor cocktail (without EDTA, Sigma-Aldrich product no. S8830) at a concentration of 0.35 g of cell pellet/mL of buffer.

Bacterial cell lysis was achieved by homogenization utilizing a French pressure cell press (SLM Aminco FA-078, high ratio, gage pressure of 1260) and a French pressure cell (Thermo FA-032, 1 in. piston diameter, cell pressure of 20000 psi). Each 25−30 mL batch of bacterial cell suspension was processed twice. Additional cell lysis was accomplished by sonication on ice utilizing a Fisher Scientific Sonic Dismembrator 550 equipped with a microtip (Fisher Scientific, Pittsburgh, PA). The sonication conditions were as follows: setting 4, total processing time of 15 min, on time of 15.0 s, and off time of 15.0 s. Insoluble cell debris was removed by centrifugation (JA-25.50 rotor, 40000*g*, 20 min, 4 °C). The supernatant was slowly brought to 65% saturation by being stirred at 4 °C using solid ammonium sulfate. After addition of all the ammonium sulfate, the protein suspension was stirred slowly at 4 °C for 12 h. Insoluble material was removed by centrifugation (JA25.50 rotor, 40000*g*, 20 min, 4 °C). The supernatant was desalted at 4 °C by chromatography through a Sephadex G-25 (GE Healthcare, Piscataway, NJ) column using NPND buffer (pH 7.4) as the mobile phase. DNA was precipitated from the desalted protein solution using protamine sulfate [0.1% (w/v)]. The protamine sulfate was added slowly while the mixture was being stirred at 4 °C, and this mixture was allowed to stir slowly at 4 °C for 12 h. Insoluble material was removed by centrifugation as described above. The supernatant was concentrated by ultrafiltration utilizing an Amicon stirred cell (model 402) at 4 °C (Millipore Ultrafiltration Membrane, Regenerated Cellulose, 76 mm diameter, NMWL of 1000 Da).

The concentrated protein solutions were buffer-exchanged into HisTrap binding buffer [20 mM sodium phosphate (pH 7.4), 0.5 M NaCl, and 30 mM imidazole] utilizing PD MidiTrap G-25 columns (GE Healthcare) as per the manufacturer's directions. The buffer-exchanged protein mixture was loaded onto a HisTrap FF (GE Healthcare) column at 25 °C pre-equilibrated with HisTrap binding buffer. The column was washed extensively with HisTrap binding buffer; the column was eluted with HisTrap elution buffer [20 mM sodium phosphate (pH 7.4), 0.5 M NaCl, and 0.5 M imidazole]. The HisTrap-eluted protein was buffer-exchanged

into 50 mM sodium phosphate (pH 7.0) and 1.0 M ammonium sulfate with PD MidiTrap G-25 columns as described above and loaded onto a pre-equilibrated hydrophobic interaction column (HiTrap Phenyl HP, GE Healthcare) at 25 °C. Protein delipidation was achieved by eluting the protein from the HiTrap Phenyl HP column utilizing a linear buffer gradient from 50 mM sodium phosphate (pH 7.0) and 1.0 M ammonium sulfate to 50 mM sodium phosphate (pH 7.0). Delipidated protein was buffer-exchanged (PD MidiTrap G-25) into 20 mM sodium phosphate (pH 7.4) and 150 mM NaCl prior to His tag removal utilizing the TAGZyme Kit (Qiagen) according to the manufacturer's directions. The protein was buffer-exchanged (PD MidiTrap G-25) into HisTrap binding buffer as described above prior to being loaded onto the HisTrap FF column as described above. The column wash (unbound) and the column eluate were examined by sodium dodecyl sulfate−polyacrylamide gel electrophoresis (SDS−PAGE). All L-FABP was found in the column wash material (data not shown), indicating complete His tag removal. The purified L-FABP (~1.5 mg/L of culture) was buffer-exchanged (PD MidiTrap G-25) into 10 mM potassium phosphate (pH 7.4) and 1 mM dithiothreitol, aliquoted, and stored at −80 °C.

Purity and Identity of the Recombinant L-FABP Determined by Amino Acid Analysis and Mass Spectroscopy. Aliquots of the purified rat L-FABP as well as human WT T94T and T94A mutant L-FABPs were analyzed by amino acid analysis and matrix-assisted laser desorption time-of-flight (MALDI-TOF) mass spectrometry (L. Dangott, Protein Chemistry Laboratory, Texas A&M University) to determine protein purity (>98%), concentration, and molecular weight. Mass spectrometry was performed utilizing a Shimadzu/Kratos Axima CFR MALDI-TOF mass spectrometer in reflectron mode. The matrix used was α-cyano-4-hydroxycinnamic acid (Sigma-Aldrich), and the instrument was calibrated using cytochrome *c*.

Fluorescence Spectra for Recombinant Proteins. L-FABP tyrosine fluorescence emission spectra were recorded at 24 °C using a Varian Cary Eclipse Fluorescence Spectrophotometer (Varian, Inc., Palo Alto, CA), by scanning from 295 to 420 nm, with an excitation wavelength of 280 nm. Rat L-FABP and human L-FABP have three tyrosines and one tyrosine per protein molecule, respectively. To obtain emission at equivalent quantities of tyrosine, protein concentrations of 200 nM for the rat L-FABP and 600 nM for WT T94T and T94A were used.

Circular Dichroism Spectroscopy To Determine Recombinant Protein Secondary Structure. All CD spectroscopy experiments were performed utilizing a JASCO J-815 CD spectrometer (JASCO, Easton, MD) equipped with a model PFD-425S Peltier type FDCD attachment for temperature regulation. All experiments (temperature and ligand interaction) were conducted at a final protein concentration of 0.5 μM as determined by amino acid analysis (see above) in a buffer containing 10 mM potassium phosphate (pH 7.4) with or without 1% ethanol. The presence of ethanol was determined to have no effect on ligand binding, protein CD spectra, or resulting secondary structure determinations (data not shown). Each protein sample was incubated while being stirred (250 rpm) at 25 °C for 10 min prior to being scanned. The sample was scanned 10 times from 185 to 250 nm. The final CD spectrum obtained represented an average of 10 scans; the spectrum was background-subtracted, and the spectrum was mathematically smoothed using the Means-Movement method with a convolution width of 5. CD spectra of each protein can be found at http://pcddb.cryst.bbk.ac.uk (PCDDB ID CD000413200−PCDDB ID CD000413400). Secondary structure analysis was performed utilizing the analysis software supplied with the CD spectrometer. SDP (soluble and denatured protein) 48 was used as the reference set. Spectra were analyzed with CONTIN, CDSSTR, and SELCON 3. CONTIN consistently produced the lowest root-mean-square deviation (rmsd) of these algorithms (data not shown). The percent change in secondary structure between two protein samples was calculated using the following formula: $[(\%\ \text{secondary structure}_{\text{sample 2}} - \%\ \text{secondary structure}_{\text{sample 1}})/(\%\ \text{secondary structure}_{\text{sample 1}})] \times 100\%$.

Stability of the Recombinant Protein to Thermal Denaturation Determined by CD Spectroscopy. Temperature CD studies of rat and human L-FABPs were performed as follows. Each sample containing 0.5 μM protein in 10 mM potassium phosphate (pH 7.4) was incubated while being stirred at 25 °C for 10 min in the FDCD attachment, and then CD spectra were obtained as described above. The sample temperature was increased by 10 °C at a rate of 1 °C/min followed by a 10 min incubation prior to obtaining the CD spectrum. This procedure was repeated until the final sample analysis was performed as described at 95 °C. Upon completion of the temperature scans, all spectra were analyzed, and secondary structure determinations were performed as described above.

Ligand Binding As Assessed by the ANS Fluorescence Displacement Assay. ANS is very weakly fluorescent in buffer, but its fluorescence increases upon binding to the L-FABP. Therefore, ANS was excited at 380 nm, and emission spectra were recorded by scanning from 410 to 600 nm. Two types of titrations were performed. First, the L-FABP (500 nM) was titrated with ANS (0−48 μM, forward titration). Second, ANS (100 nM) was titrated with increasing amounts of the L-FABP (0−4 μM, reverse titration). The fluorescence intensity of ANS (per nanomolar) when it was fully bound to the L-FABP was calculated by curve fitting the reverse titration curve. This parameter was then used in forward titration to calculate the fractional saturation and free ANS concentration. K_d and B_{max} were determined from the binding curve of fractional saturation (Y) versus free ANS concentration (X).

The binding affinity of the ligand (phytanic acid, fenofibrate, and fenofibric acid) for the L-FABP was determined by the ANS displacement assay. A solution of the L-FABP (500 nM) and ANS (35 μM) was titrated with phytanic acid (0−6.4 μM) or fenofibrate (0−6 μM for the rat L-FABP and 0−4 μM for the human L-FABP) or fenofibric acid (0−300 μM for the rat L-FABP and 0−48 μM for the human L-FABP). EC_{50} was obtained from the displacement curve. K_i was calculated from the equation $EC_{50}/[ANS] = K_i/K_d$.

Impact of Ligand Binding on Recombinant Protein Secondary Structure Determined by CD. Each sample contained 0.5 μM protein in 10 mM potassium phosphate (pH 7.4). Ligand (phytanic acid, fenofibrate, or fenofibric acid) was added from a stock solution of 500 μM ligand in ethanol such that the final ligand concentration was 5 μM and the final ethanol concentration was 1%. The protein/ligand sample was incubated while being stirred at 25 °C for 10 min in the FDCD attachment prior to obtaining the CD spectrum. Again, the final CD spectrum was an average of 10 scans and was background-subtracted (buffer/ligand/ethanol) and mathematically smoothed, and the secondary structure content was determined as described above. The percent change in secondary structure

between two protein samples was calculated using the following formula: [(% secondary structure$_{sample\ 2}$ − % secondary structure$_{sample\ 1}$)/(% secondary structure$_{sample\ 1}$)] × 100%.

Fenofibrate-Mediated Induction of Transcription of PPARα-Regulated Proteins in Cultured Primary Human Hepatocytes As Assessed by Quantitative Real-Time Polymerase Chain Reaction. Cryopreserved primary human hepatocytes from female (50 ± 3 years old) Caucasian donors were from Life Technologies. Hepatocytes were genotyped to determine WT T94T (TT), heterozygous (TC), or T94A (CC) variant expression as described in refs 45 and 46, thawed, plated, and cultured overnight according to the supplier's protocol (Life Technologies). Human hepatocytes were then incubated with 40 μM BSA (fatty acid free) or 40 μM BSA−fenofibrate (1:1, mol/mol) complex for 24 h in medium prepared by adding 6 mM glucose, 100 nM insulin, and 10 nM dexamethasone to glucose free William's E medium (US Biological, Salem, MA). Total mRNA was obtained with the RN-easy kit from Qiagen and the RN-ase free DNase set from Qiagen GmbH (Hilden, Germany). TaqMan, One-Step RT-PCR Master Mix reagents, and TaqMan Gene Expression Assays for human mRNAs were from Applied Biosystems (by Life Technologies): liver fatty acid binding protein (L-FABP), fatty acid transport protein-5 (FATP5), and peroxisome proliferator activated receptor α (PPAR-α). Messenger RNA levels were determined according to the procedures provided by the manufacturer.

Statistics. Statistical analysis was performed by one-way analysis of variance (ANOVA) combined with the Newman−Keuls multiple-comparison post test (GraphPad Prism version 3.03, GraphPad, San Diego, CA). Unless otherwise noted, data are expressed as means ± the standard error of the mean (n = 4−6) and P is indicated as described in the figure legends. Graphical analysis was accomplished using SigmaPlot 2002 for Windows version 8.02 (SPSS, Chicago, IL).

RESULTS

Amino Acid Sequence Homology among Rat, Human WT T94T, and Human T94A Variant L-FABPs. Human and murine L-FABPs mediate ligand signaling to their respective PPARαs.[12,21,22,24,27,58] However, mRNA profiling of rodent (rat and mouse) and human hepatocytes revealed significant differences in responses to fibrates.[59−61] While this was attributed primarily to species differences in PPARα, species differences in L-FABPs must also be considered. While rat[10,62] and human[13,14] L-FABPs share significant overall secondary structure, each having a 10-β-sheet β-barrel along with two α-helices and turns between them, differences in their 127-amino acid sequence suggest significant influences on secondary structures. The human WT L-FABP contains 13 (T94T in both rat and human WT L-FABPs) nonconservative (Figure 1, red) and 9 conservative (Figure 1, green) substitutions such that it is only 82.7% identical and 89.8% similar to the rat L-FABP.[63] Consequently, human L-FABPs have three fewer basic (positively charged) amino acids than the rat L-FABP, and the resultant pI, calculated as described previously,[63] for the human WT T94T L-FABP is 6.60, considerably more acidic than that of the rat L-FABP (pI of 7.79). While the human L-FABP T94A variant also has a pI of 6.60, this substitution results in replacement of a medium-sized, polar, uncharged T residue with a smaller, nonpolar, aliphatic A residue (Figure 1, asterisk). The consequences of these differences with respect to the human L-FABP structure, stability, ligand binding, and function are detailed in the following sections.

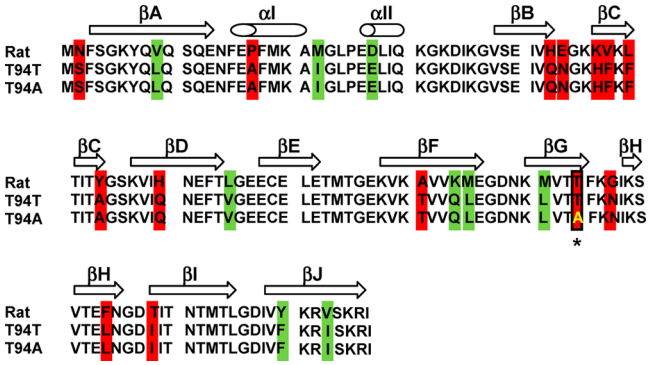

Figure 1. Amino acid sequence alignment of rat, human WT T94T, and human T94A variant L-FABPs. Multiple-sequence alignment was performed utilizing Clustal W (http://embnet.vital-it.ch/software/ClustalW.html). Additional evaluation of amino acid substitutions was performed utilizing information from ref 63. Protein secondary structural elements are pictured above the aligned sequences; α-helices αI and αII designated by cylindrical cones and β-sheets βA−βJ designated by arrows. Conservative amino acid substitutions are highlighted in green. Nonconservative amino acid substitutions are highlighted in red. The T94A amino acid substitution in the human L-FABP is denoted with an asterisk.

Purification of Recombinant Human WT T94T and T94A Variant L-FABPs. Because all previously described human L-FABP cDNAs were of the human WT T94T L-FABP,[52−54] it was necessary to prepare the T94A variant L-FABP as well as the WT T94T L-FABPs. Sequencing of a commercially available cDNA encoding the human L-FABP revealed that it encoded the T94A variant L-FABP. Therefore, the WT T94T L-FABP was obtained by site-directed mutagenesis of T94A L-FABP variant cDNA as described in Experimental Procedures. Respective cDNAs were inserted into a bacterial expression vector for protein expression and purification (Figure 2A) also as detailed in Experimental Procedures. Purified WT T94T and T94A variant L-FABPs were detected as single bands on SDS−PAGE gels (Figure 2B,D, lane 11). MALDI-TOF analysis of the final, the His tag free human WT T94T L-FABP and T94A L-FABP variant detected main mass peaks at 14208.5 Da (Figure 2C) and 14178.39 Da (Figure 2E), respectively, consistent with molecular masses based on amino acid sequence (Figure 1). Increasing the amount of the L-FABP loaded on the SDS−PAGE gel did not reveal significant additional bands (Figure 2F). Thus, these proteins were sufficiently pure (>98%) for structural and functional characterization.

Tyrosine Fluorescence Spectroscopy of Rat and Human L-FABPs. The human WT T94T L-FABP has a single Tyr residue at Y7, located in βA (part of the β-barrel ligand binding structure, N-terminal to the α-helical cap),[10] but it is not known if the T94A substitution altered the polarity of the microenvironment wherein this Tyr residue resides. Although both WT T94T and T94A L-FABPs had maximal fluorescence emission at 305 nm, the fluorescence efficiency of Tyr in both human L-FABPs was ∼4-fold lower than that of Tyr in the rat L-FABP (not shown). While this suggested significant differences between rat and human L-FABP Tyr microenvironments, the T94A substitution did not alter this microenvironment.

dx.doi.org/10.1021/bi401014k | Biochemistry 2013, 52, 9347−9357

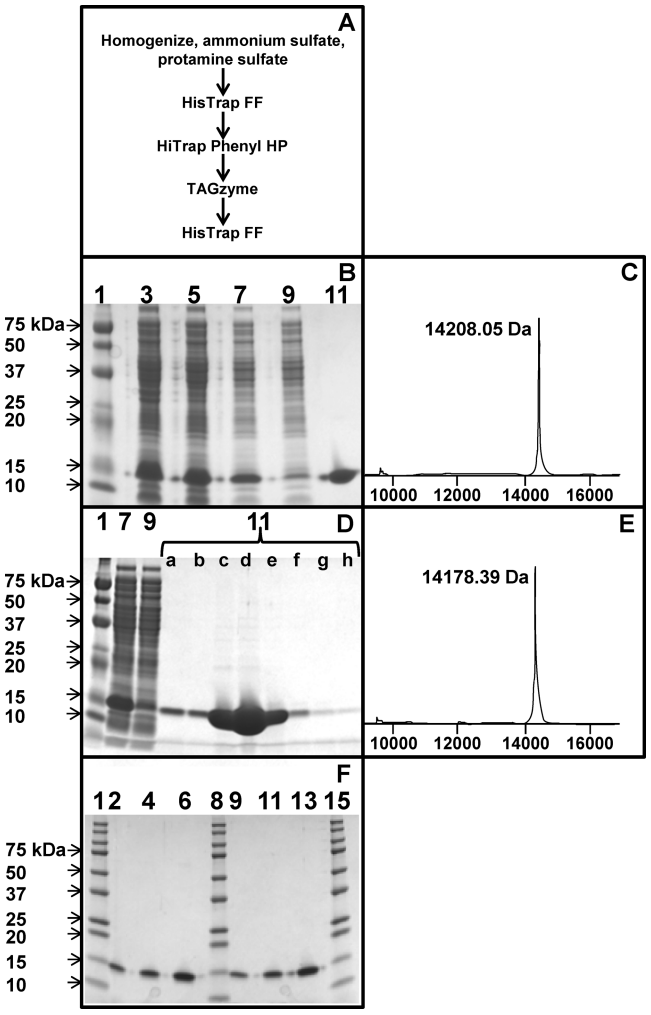

Figure 2. Purification flowchart, SDS–PAGE analysis, and mass spectra of human WT T94T and T94A variant L-FABPs. (A) Outline of the human L-FABP purification procedure. Aliquots of the human WT T94T L-FABP (B and C) and the T94A variant L-FABP (D and E) were examined by SDS–PAGE and mass spectrometry as described in Experimental Procedures. (B) SDS–PAGE analysis of the WT T94T human L-FABP: lane 1, molecular mass markers; lane 3, cell homogenate; lane 5, cell homogenate supernatant; lane 7, ammonium sulfate/protamine sulfate supernatant; lane 9, HisTrap FF column wash (unbound); lane 11, HisTrap FF column eluate. (C) MALDI-TOF analysis of the human WT T94T L-FABP after delipidation and His tag removal. (D) SDS–PAGE analysis of the human T94A variant L-FABP: lane 1, molecular mass markers; lane 7, ammonium sulfate/protamine sulfate supernatant; lane 9, HisTrap FF column wash (unbound); lanes 11a-h, HisTrap FF column elution fractions. (E) MALDI-TOF analysis of the human L-FABP T94A variant after delipidation and His tag removal. (F) SDS–PAGE analysis of the purified WT T94T L-FABP (lane 2, 1 μg of protein; lane 4, 2 μg of protein; lane 6, 5 μg of protein) and T94A variant L-FABP (lane 9, 1 μg of protein; lane 11, 2 μg of protein; lane 13, 5 μg of protein). Lanes 1, 8, and 15 contained molecular mass markers.

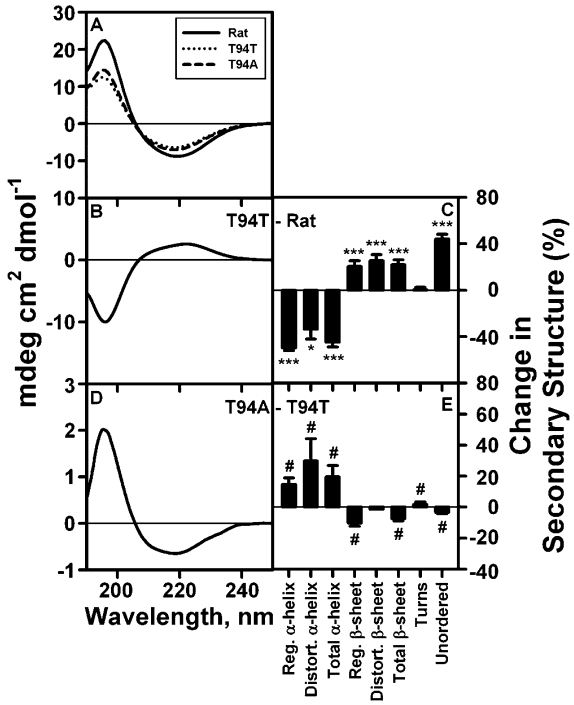

Figure 3. CD spectra and secondary structures of rat and human L-FABPs. Rat and human L-FABPs were examined by CD spectroscopy, and secondary structures were determined as described in Experimental Procedures. (A) Representative CD spectra of 0.5 μM rat, human WT T94T, and human T94A variant L-FABPs at 25 °C. (B) Difference CD spectrum (human WT T94T minus rat). (C) Percent change in secondary structure (human WT T94T minus rat). (D) Difference CD spectrum (T94A variant minus WT T94T). (E) Percent change in secondary structure (T94A variant minus WT T94T). *P < 0.05 for human T94T vs rat secondary structure. ***P < 0.001 for human T94T vs rat secondary structure. #P < 0.05 for T94A vs T94T secondary structure.

Secondary Structure of Rat and Human L-FABPs. CD spectra of rat and human L-FABPs (Figure 3A) all displayed maxima and minima near 195 and 220 nm. As shown by T94T minus rat L-FABP difference spectra, however, the human WT T94T L-FABP had less positive molar ellipticity at the 195 nm maximum and less negative molar ellipticity at the 220 nm minimum (Figure 3B). By quantitative analysis, the human WT T94T L-FABP had less α-helix of all types but more β-sheet of all types and more unordered structure than the rat L-FABP (Figure 3C). In contrast, human T94A minus T94T difference spectra had more positive molar ellipticity at the 195 nm maximum and more negative molar ellipticity at the 220 nm minimum (Figure 3D). Quantitative analysis showed that the human T94A variant L-FABP had significantly more α-helix of all types but less regular β-sheet and unordered structures than the human WT T94T L-FABP (Figure 3E). The extent to which these differences impacted the L-FABP stability, ligand binding, and conformational response to ligands is addressed below.

Secondary Structure Stability of Rat and Human L-FABPs. Murine and human L-FABPs bind their respective PPARαs to induce structural alterations that alter coregulator recruitment and induce PPARα activation.[12,21,22,24,58] It is not known how differences between the rat and human WT T94T L-FABP and T94A variant impact folding stability that may be required for ligand transfer to and/or activation of PPARα. Rat L-FABP secondary structures were relatively stable to increasing temperature up to ~65 °C (Figure 4A,C,E,G). The human WT T94T L-FABP was more stable to unfolding, which did not occur until 85 °C [Figure 4B,D,F,H (●)]. As compared to the human WT T94T L-FABP, the T94A variant was more rapidly unfolded beginning at 65 °C [Figure 4B,D,F,H (○)]. On the basis of the thermally induced increase in the unordered structure content, the stability of the three L-FABPs decreased

dx.doi.org/10.1021/bi401014k | *Biochemistry* 2013, 52, 9347–9357

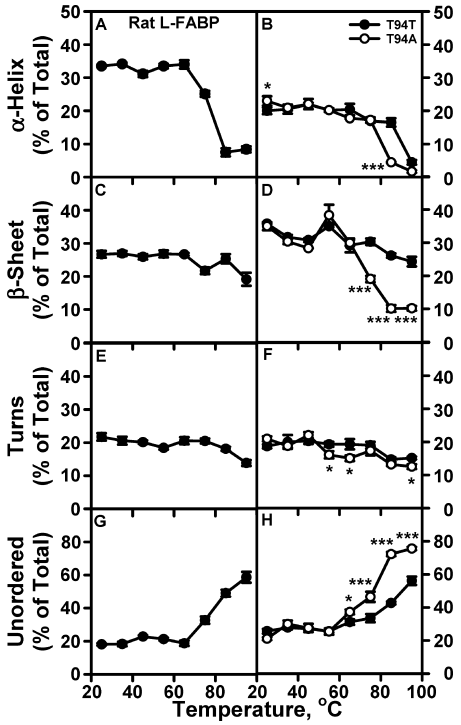

Figure 4. Sensitivity of rat and human L-FABP secondary structure to temperature-induced unfolding. CD spectra and secondary structure analysis of rat and human L-FABPs were determined as a function of sample temperature as described in Experimental Procedures. Panels A, C, E, and G show the amount of rat L-FABP total α-helix, total β-sheet, turn, and unordered secondary structure, respectively, as a percentage of the total secondary structure. Panels B, D, F, and H show the amount of human WT T94T L-FABP (●) or human T94A variant L-FABP (○) total α-helix, total β-sheet, turn, and unordered secondary structure, respectively, as a percentage of the total secondary structure. *P < 0.05 for T94A vs T94T. ***P < 0.001 for T94A vs T94T.

in the following order: human WT T94T [Figure 4H (●)] > rat (Figure 4G) > human T94A [Figure 4H (○)]. These findings with human and rat L-FABPs may contribute, in part, to the species differences in PPARα transcriptional regulation.[61]

Ligand Binding Specificity of Rat, Human WT T94T, and Human T94A Variant L-FABPs Determined by ANS Fluorescence Displacement. While the T94A substitution has been hypothesized to abolish binding of ligand to the human L-FABP, this has not been shown.[56] Phytanic acid, a naturally occurring branched-chain fatty acid from which less toxic fibrate analogues were subsequently developed,[64,65] displaced ANS from all three L-FABPs (Figure 5A) with similar K_i values (Table 1). Fenofibrate and fenofibric acid are the most commonly prescribed fibrates in the United States and Canada.[51] However, fibrate binding differed markedly among the three L-FABPs (Figure 5B,C and Table 1). (i) The rat L-FABP bound fenofibrate and fenofibric acid nearly 3- and 150-fold more weakly, respectively, than phytanic acid. (ii) The human WT T94T L-FABP and T94A variant bound fenofibrate 20-fold more strongly than fenofibric acid. (iii) The human WT T94T L-FABP and T94A bound fenofibrate with 7-fold higher affinity than rat L-FABP. (iv) The human WT T94T L-FABP and T94A variant bound fenofibric acid more strongly with >20-fold higher affinity than rat L-FABP. Thus, the T94A form did not abolish or alter binding of phytanic acid, fenofibrate, or fenofibric acid, all potent PPARα agonists.[16,66−69] Further, rat and human L-FABPs differed significantly in their ability to bind these ligands.

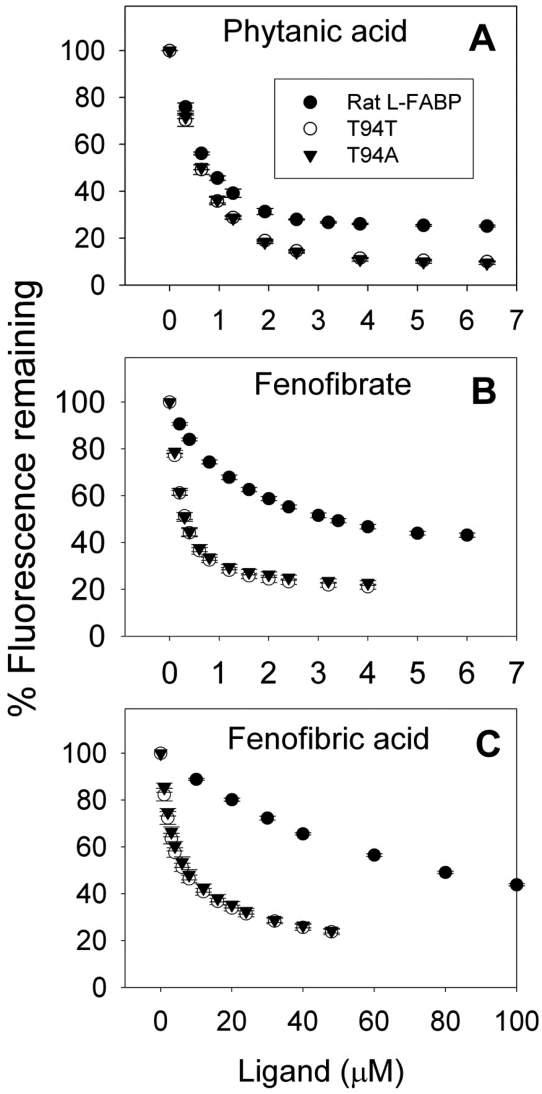

Figure 5. Binding of ligand to rat and human L-FABPs determined by ANS displacement. Displacement curves of phytanic acid (A), fenofibrate (B), and fenofibric acid (C) of L-FABP-bound ANS were obtained as described in Experimental Procedures (L-FABP, 500 nM; ANS, 35 μM): (●) rat L-FABP, (○) human WT T94T L-FABP, and (▼) human T94A variant L-FABP. All data are means ± the standard error (n = 4 or 5).

Table 1. Comparison of ANS Displacement Coefficients of Phytanic Acid and Fibrates from Murine and Human L-FABPs[a]

	ANS displacement K_i (μM)[b]		
ligand	rat L-FABP	T94T	T94A
phytanic acid	0.037 ± 0.002	0.035 ± 0.003	0.038 ± 0.02
fenofibrate	0.10 ± 0.01[d]	0.015 ± 0.001[c,d]	0.015 ± 0.001[c,d]
fenofibric acid	5.8 ± 0.5[d,e]	0.25 ± 0.03[c,d,e]	0.31 ± 0.03[c,d,e]

[a] K_i values were obtained by analysis of multiple ANS displacement curves similar to those in Figure 5 as described in Experimental Procedures. [b] Values represent means ± the standard error (n = 3−5). [c] P < 0.05 vs rat L-FABP. [d] P < 0.05 vs phytanic acid. [e] P < 0.05 vs fenofibrate.

dx.doi.org/10.1021/bi401014k | Biochemistry 2013, 52, 9347−9357

Ligand Binding Differentially Altered the Rat, Human WT T94T, and Human T94A Variant L-FABP Secondary Structure. Ligand-induced conformational changes in the L-FABP may significantly impact the α-helical portal region, interaction with PPARα, and possibly transfer of activating ligand to PPARα.[12] However, the impact of ligand binding on rat L-FABP secondary structure was modest (5−10% change) and highly specific for each ligand. For example, phytanic acid stabilized the regular α-helical region of the rat L-FABP (Figure 6A), while fenofibrate and its active metabolite fenofibric acid

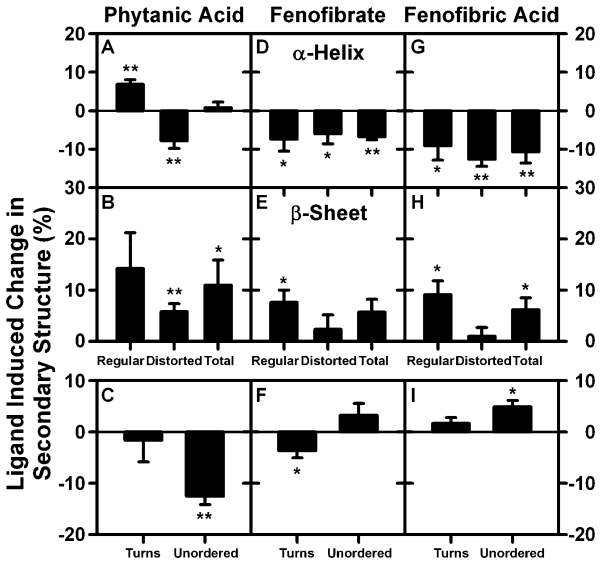

Figure 6. Changes in rat L-FABP secondary structure upon interaction with phytanic acid, fenofibrate, or fenofibric acid. The rat L-FABP (0.5 μM), with or without 5 μM ligand, was examined by CD spectroscopy and subsequent secondary structure analysis as described in Experimental Procedures. Panels A (α-helix), B (β-sheet), and C (turn and unordered) show the percent change in secondary structure (L-FABP/ligand minus L-FABP only) induced by the interaction of phytanic acid with the rat L-FABP. Panels D (α-helix), E (β-sheet), and F (turn and unordered) show the percent change in secondary structure (L-FABP/ligand minus L-FABP only) induced by the interaction of fenofibrate with the rat L-FABP. Panels G (α-helix), H (β-sheet), and I (turn and unordered) show the percent change in secondary structure (L-FABP/ligand minus L-FABP only) induced by the interaction of fenofibric acid with rat L-FABP. *P < 0.05 for L-FABP/ligand secondary structure vs L-FABP only secondary structure. **P < 0.01 for L-FABP/ligand secondary structure vs L-FABP only secondary structure.

did not (Figure 6D,G). Consistent with this finding, phytanic acid (Figure 6C) but not fenofibrate or fenofibric acid (Figure 6F,I) decreased the proportion of unordered structure in the rat L-FABP. However, all three ligands similarly altered rat L-FABP β-sheet structures (Figure 6B,E,H).

In contrast, these ligands more dramatically (10−35%) and differentially altered human WT T94T and T94A variant L-FABP secondary structures. Phytanic acid binding similarly altered the secondary structure of the human WT T94T and T94A variant L-FABP (Figure 7A−C). In contrast, the fibrate ligands differentially altered human WT T94T L-FABP secondary structure, quantitatively and with regard to fibrate specificity (Figure 7, black bars). For example, fenofibrate had little, if any, effect on the proportion of α-helix in the human WT T94T L-FABP (Figure 7D), modestly increased the proportion of β-sheet (Figure 7E) and turn (Figure 7F), and

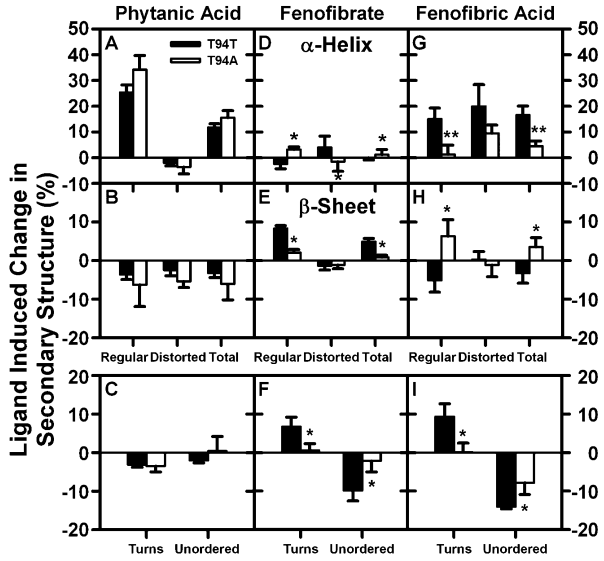

Figure 7. Impact of the T94A substitution on the secondary structural response of the human L-FABP to phytanic acid, fenofibrate, or fenofibric acid. Human WT T94T and T94A variant L-FABPs (0.5 μM) were examined by CD spectroscopy and subsequent secondary structure analysis in the absence or presence of 5 μM phytanic acid, fenofibrate, or fenofibric acid as described in Experimental Procedures. Panels A (α-helix), B (β-sheet), and C (turn and unordered) show the percent change in secondary structure (L-FABP/ligand minus L-FABP only) upon the interaction of phytanic acid with the human L-FABP. Panels D (α-helix), E (β-sheet), and F (turn and unordered) show the percent change in secondary structure (L-FABP/ligand minus L-FABP only) upon the interaction of fenofibrate with the human L-FABP. Panels G (α-helix), H (β-sheet), and I (turn and unordered) show the percent change in secondary structure (L-FABP/ligand minus L-FABP only) upon the interaction of fenofibric acid with the human L-FABP. *P < 0.05 for T94A L-FABP/ligand secondary structure vs T94T L-FABP/ligand secondary structure. **P < 0.01 for T94A L-FABP/ligand secondary structure vs T94T L-FABP/ligand secondary structure.

decreased significantly the proportion of unordered (Figure 7F) structure. In contrast, the active metabolite fenofibric acid markedly increased the proportion of α-helix (Figure 7G) and turns (Figure 7I), modestly decreased the proportion of β-sheet (Figure 7H), and significantly decreased the proportion of unordered (Figure 7I) structure.

The T94A substitution in the human T94A variant L-FABP significantly altered the ability of fenofibrate and fenofibric acid to impact secondary structure. As compared to its effect on the human WT T94T L-FABP, fenofibrate modestly increased proportions of α-helix (Figure 7D) and β-sheet (Figure 7E) while somewhat decreasing the proportion of unordered structure (Figure 7F). The human T94A substitution weakened the ability of fenofibric acid to affect the proportion of α-helical structure (Figure 7G), increased the proportion of β-sheet (Figure 7H), and decreased the proportion of unordered structure (Figure 7I).

T94A Expression Impaired Fenofibrate-Mediated Transcription of PPARα-Regulated Proteins in Primary Human Hepatocytes. The human T94A variant L-FABP exhibited an altered conformational response to fenofibric acid, the active metabolite of fenofibrate (Figure 7). Therefore, the functional impact of fenofibrate was examined in cultured primary human hepatocytes that had been genotyped and segregated into homozygous WT T94T L-FABP (TT),

dx.doi.org/10.1021/bi401014k | *Biochemistry* 2013, 52, 9347−9357

heterozygous T94T/T94A (TC), and homozygous T94A variant (CC) L-FABP expressors as described in Experimental Procedures. T94A-expressing hepatocytes exhibited an impaired response to fenofibrate-mediated transcription of PPARα-regulated proteins: PPARα itself, L-FABP, and FATP5 (Figure 8). Taken together, these findings indicated

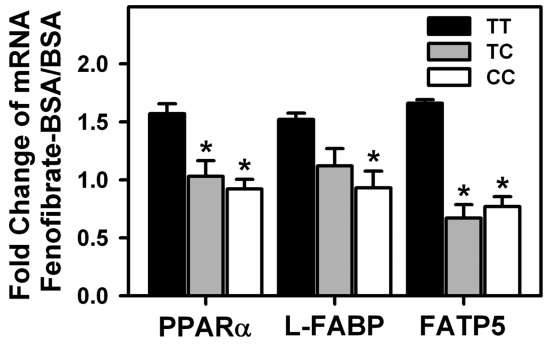

Figure 8. Effect of T94A on ligand-induced transcription of PPARα-regulated proteins. Primary human hepatocytes were treated as described in Experimental Procedures and then incubated for 24 h with fatty acid free BSA (Alb) or a BSA/fenofibrate mixture (40 μM, FF) in 6 mM glucose-containing medium as described previously.[30,31] Quantitative real-time (rt) PCR for human PPARα, L-FABP, and FATP5 determined mRNA levels that were normalized to an internal control (18S RNA). Values show the fold change induced by the FF/alb complex relative to albumin only. All data are means ± the standard error (n = 8−10 in each group). *P < 0.05 for homozygous (CC) or heterozygous (TC) T94A variants vs WT T94T (TT).

that the T94A substitution not only altered the structure and structural response to fibrate binding but also weakened its ability to function in mediating fibrate signaling to PPARα.

DISCUSSION

Although both murine and human liver fatty acid binding proteins (L-FABPs) were cloned nearly 30 years ago, subsequent progress focused primarily on resolving the structure[10,11,19,62,70] and function (reviewed in refs 2 and 3) of the murine L-FABP. More recent studies have begun to examine the tertiary structure[14,38,39,41,42,71,72] and xenobiotic ligand (fibrate, phthalates, and phenoxy herbicides) binding specificity[12,40] of the human WT T94T L-FABP. Although a highly common SNP in the human L-FABP coding sequence results in a single-amino acid substitution, T94A, almost nothing is known about its impact on the structure, ligand binding affinity, or function.[43,44] Studies herein provide new insights.

First, rat and human WT T94T L-FABPs differed significantly in secondary structure, structural stability, fibrate binding affinity and specificity, and conformational response. Furthermore, the human L-FABPs exhibited much greater affinity for fibrates than the rat L-FABP. In contrast, there was no difference in affinities for phytanic acid, the naturally occurring fatty acid from which less toxic fibrate analogues were first developed.[64,65] Transcriptional profiling studies also demonstrated significant species differences in the induction of mRNA by PPARα agonists in cultured rat, mouse, and human primary hepatocytes.[59−61] These findings underscore the need for structure−activity studies with human and rat L-FABPs.

Second, the T94A substitution in the human L-FABP significantly altered the secondary structure and decreased its stability with respect to unfolding. CD spectral analysis is less sensitive to β-sheet structure and therefore overestimates the proportion of α-helix in the human L-FABP [~20% (Figure 4)] as compared to that determined by NMR or X-ray (~12%).[14,62,72] Nevertheless, there are clear differences between the human WT T94T L-FABP and T94A variant L-FABPs. The T94A substitution increased the proportion of α-helical structure and concomitantly decreased the thermal stability of the human L-FABP by nearly 10 °C (from 85 to 65−75 °C). Interestingly, an earlier infrared spectroscopic study of the native human L-FABP isolated from liver of an unknown phenotype showed that above 65−75 °C the proportion of α-helix and β-sheet significantly decreased.[73] This suggests that the latter native human L-FABP may have been isolated from an individual expressing the T94A variant L-FABP. Structural differences can impact the interaction of the L-FABP with other proteins as evidenced by L-FABP conformers differentially enhancing bound LCFA-CoA utilization by microsomal glycerol-3-phosphate acyltransferase (GPAT).[74−76] Likewise, while single-amino acid substitutions in the cytosolic domain of carnitine palmitoyl acyltransferase-1A (CPT1A, the rate-limiting enzyme in fatty acid β-oxidation) do not alter ligand binding affinity, they significantly alter the secondary structure and inhibit binding of the L-FABP to thereby inhibit mitochondrial fatty acid β-oxidation.[77]

Third, although the T94A substitution in the human L-FABP did not alter the affinity for potent PPARα agonists (phytanic acid, fenofibrate, and fenofibric acid), the T94A substitution weakened the ability of fibrate ligands (especially fenofibric acid) to alter the secondary structure of the human L-FABP.

Fourth, T94A expression in cultured primary human hepatocytes significantly impaired fenofibrate-mediated transcription of PPARα-regulated proteins such as FATP5. The L-FABP directly interacts with FATP5 at the mouse hepatocyte plasma membrane, suggesting that this interaction may facilitate ligand uptake.[78] Indeed, L-FABP overexpression enhances the uptake of phytanic acid and other fatty acids, while L-FABP gene ablation inhibits uptake in cultured cells, in mouse hepatocytes, and *in vivo*.[35,78−80] Whether the T94A substitution impacts fenofibrate uptake is unknown, but fenofibrate has been reported to be less effective in lowering elevated plasma triglyceride levels to basal levels in L-FABP T94A variant human subjects.[44]

In summary, the T94A substitution in the human L-FABP significantly altered the secondary structure, stability, conformational response to fibrate binding, and fenofibrate activation of PPARα transcriptional activity in human hepatocytes. Fibrate binding induces the redistribution of the L-FABP into nuclei for interaction with and activation of PPARα in mouse primary hepatocytes.[30] Within the nucleus, the L-FABP binds PPARα,[12,21,22] likely to facilitate ligand transfer,[12] and induces PPARα transcription of multiple proteins in fatty acid metabolism in mouse primary hepatocytes.[24,28−31,81] The net effect of these actions is to lower plasma triglyceride levels,[69,82−89] primarily by inducing hepatic PPARα transcription of proteins in long-chain fatty acid (LCFA) uptake[59,60,90,91] and β-oxidation[59,60,82] as well as extrahepatic PPARα-regulated proteins in plasma VLDL triglyceride hydrolysis.[59,60,92] While the impact of the human L-FABP T94A substitution on these pathways remains to be resolved, our findings of altered conformation and conformational

dx.doi.org/10.1021/bi401014k | *Biochemistry* 2013, 52, 9347−9357

response to fibrate binding suggest a significant influence. Finally, the data presented herein indicate that the human L-FABP T94A variant represents an altered-function rather than abolition-of-function mutation. In contrast, L-FABP gene ablation completely abolishes the contribution of L-FABP to ligand binding as well as the ability of fibrates (fenofibrate and bezafibrate) to induce PPARα transcriptional activity only in murine hepatocytes.[30]

AUTHOR INFORMATION

Corresponding Author

*Department of Physiology and Pharmacology, Texas A&M University, TVMC, College Station, TX 77843-4466. E-mail: fschroeder@cvm.tamu.edu. Phone: (979) 862-1433. Fax: (979) 862-4929.

Funding

This work was supported by National Institutes of Health Grants DK41402 (F.S. and A.B.K.) and DK70965 (B.P.A.).

Notes

The authors declare no competing financial interest.

ABBREVIATIONS

CD, circular dichroism; ANS, 1-anilinonaphthalene-8-sulfonic acid; FF, fenofibrate; FA, fenofibric acid; L-FABP or FABP1, liver fatty acid binding protein; WT T94T, wild-type human L-FABP; L-FABP T94A, human L-FABP T94A variant; LCFA, long-chain fatty acid; PPARα, -β/δ, or -γ, peroxisome proliferator-activated receptor α, β/δ, or γ, respectively; SNP, single-nucleotide polymorphism.

REFERENCES

(1) Ockner, R. K., Manning, J. A., Poppenhausen, R. B., and Ho, W. K. (1972) A binding protein for fatty acids in cytosol of intestinal mucosa, liver, myocardium, and other tissues. *Science 177*, 56−58.

(2) Atshaves, B. P., Martin, G. G., Hostetler, H. A., McIntosh, A. L., Kier, A. B., and Schroeder, F. (2010) Liver fatty acid binding protein (L-FABP) and dietary obesity. *J. Nutr. Biochem. 21*, 1015−1032.

(3) Storch, J., and Corsico, B. (2008) The emerging functions and mechanisms of mammalian fatty acid binding proteins. *Annu. Rev. Nutr. 28*, 18.1−18.23.

(4) Thompson, J., Reese-Wagoner, A., and Banaszak, L. (1999) Liver fatty acid binding protein: Species variation and the accomodation of different ligands. *Biochim. Biophys. Acta 1441*, 117−130.

(5) Miller, K. R., and Cistola, D. P. (1993) Titration calorimetry as a binding assay for lipid-binding proteins. *Mol. Cell. Biochem. 123*, 29−37.

(6) Rolf, B., Oudenampsen-Kruger, E., Borchers, T., Faergeman, N. J., Knudsen, J., Lezius, A., and Spener, F. (1995) Analysis of the ligand binding properties of recombinant bovine liver-type fatty acid binding protein. *Biochim. Biophys. Acta 1259*, 245−253.

(7) Richieri, G. V., Ogata, R. T., and Kleinfeld, A. M. (1994) Equilibrium constants for the binding of fatty acids with fatty acid binding proteins from adipocyte, intestine, heart, and liver measured with the flourscent probe ADIFAB. *J. Biol. Chem. 269*, 23918−23930.

(8) Frolov, A., Cho, T. H., Murphy, E. J., and Schroeder, F. (1997) Isoforms of rat liver fatty acid binding protein differ in structure and affinity for fatty acids and fatty acyl CoAs. *Biochemistry 36*, 6545−6555.

(9) Wolfrum, C., Borchers, T., Sacchettini, J. C., and Spener, F. (2000) Binding of fatty acids and perooxisome proliferators to orthologous fatty acid binding proteins from human, murine, and bovine liver. *Biochemistry 39*, 1469−1474.

(10) He, Y., Yang, X., Wang, H., Estephan, R., Francis, F., Kodukula, S., Storch, J., and Stark, R. E. (2007) Solution-state molecular structure of apo and oleate-liganded liver fatty acid binding protein. *Biochemistry 46*, 12543−12556.

(11) Chuang, S., Velkov, T., Horne, J., Wielens, J., Chalmers, D. K., Porter, C. J. H., and Scanlon, M. J. (2009) Probing fibrate binding specificity of rat liver fatty acid binding protein. *J. Med. Chem. 52*, 5344−5355.

(12) Velkov, T. (2013) Interactions between human liver fatty acid binding protein and peroxisome proliferator activated receptor drugs. *PPAR Res.*, DOI: doi.org/10.1155/2013/938401.

(13) Sharma, A., and Sharma, A. (2011) Fatty acid induced remodeling within the human liver fatty acid binding protein. *J. Biol. Chem. 286*, 31924−31928.

(14) Cai, J., Lucke, C., Chen, Z., Qiao, Y., Klimtchuk, E., and Hamilton, J. A. (2012) Solution structure and backbone dynamics of human liver fatty acid binding protein: Fatty acid binding revisited. *Biophys. J. 102*, 2585−2594.

(15) Frolov, A., Miller, K., Billheimer, J. T., Cho, T.-C., and Schroeder, F. (1997) Lipid specificity and location of the sterol carrier protein-2 fatty acid binding site: A fluorescence displacement and energy transfer study. *Lipids 32*, 1201−1209.

(16) Wolfrum, C., Ellinghaus, P., Fobker, M., Seedorf, U., Assmann, G., Borchers, T., and Spener, F. (1999) Phytanic acid is ligand and transcriptional activator of murine liver fatty acid binding protein. *J. Lipid Res. 40*, 708−714.

(17) Hanhoff, T., Benjamin, S., Borchers, T., and Spener, F. (2005) Branched-chain fatty acids as activators of peroxisome proliferators. *Eur. J. Lipid Sci. Technol. 107*, 716−729.

(18) Maatman, R. G., van Moerkerk, H. T., Nooren, I. M., van Zoelen, E. J., and Veerkamp, J. H. (1994) Expression of human liver fatty acid-binding protein in *Escherichia coli* and comparative analysis of its binding characteristics with muscle fatty acid-binding protein. *Biochim. Biophys. Acta 1214*, 1−10.

(19) Chuang, S., Velkov, T., Horne, J., Porter, C. J. H., and Scanlon, M. J. (2008) Characterization of the drug binding specificity of rat liver fatty acid binding protein. *J. Med. Chem. 51*, 3755−3764.

(20) Kanda, T., Ono, T., Matsubara, Y., and Muto, T. (1990) Possible role of rat fatty acid binding proteins in the intestine as carriers of phenol and phthalate derivatives. *Biochem. Biophys. Res. Commun. 168*, 1053−1058.

(21) Hostetler, H. A., McIntosh, A. L., Atshaves, B. P., Storey, S. M., Payne, H. R., Kier, A. B., and Schroeder, F. (2009) Liver type Fatty Acid Binding Protein (L-FABP) interacts with peroxisome proliferator activated receptor-α in cultured primary hepatocytes. *J. Lipid Res. 50*, 1663−1675.

(22) Hostetler, H. A., Balanarasimha, M., Huang, H., Kelzer, M. S., Kaliappan, A., Kier, A. B., and Schroeder, F. (2010) Glucose regulates fatty acid binding protein interaction with lipids and PPARα. *J. Lipid Res. 51*, 3103−3116.

(23) Lawrence, J. W., Kroll, D. J., and Eacho, P. I. (2000) Ligand dependent interaction of hepatic fatty acid binding protein with the nucleus. *J. Lipid Res. 41*, 1390−1401.

(24) Wolfrum, C., Borrmann, C. M., Borchers, T., and Spener, F. (2001) Fatty acids and hypolipidemic drugs regulate PPARα and PPARγ gene expresion via L-FABP: A signaling path to the nucleus. *Proc. Natl. Acad. Sci. U.S.A. 98*, 2323−2328.

(25) Huang, H., Starodub, O., McIntosh, A., Kier, A. B., and Schroeder, F. (2002) Liver fatty acid binding protein targets fatty acids to the nucleus: Real-time confocal and multiphoton fluorescence imaging in living cells. *J. Biol. Chem. 277*, 29139−29151.

(26) Huang, H., Starodub, O., McIntosh, A., Atshaves, B. P., Woldegiorgis, G., Kier, A. B., and Schroeder, F. (2004) Liver fatty acid binding protein colocalizes with peroxisome proliferator receptor α and enhances ligand distribution to nuclei of living cells. *Biochemistry 43*, 2484−2500.

(27) Schroeder, F., Petrescu, A. D., Huang, H., Atshaves, B. P., McIntosh, A. L., Martin, G. G., Hostetler, H. A., Vespa, A., Landrock, K., Landrock, D., Payne, H. R., and Kier, A. B. (2008) Role of fatty acid binding proteins and long chain fatty acids in modulating nuclear receptors and gene transcription. *Lipids 43*, 1−17.

(28) McIntosh, A. L., Atshaves, B. P., Hostetler, H. A., Huang, H., Davis, J., Lyuksyutova, O. I., Landrock, D., Kier, A. B., and Schroeder,

F. (2009) Liver type fatty acid binding protein (L-FABP) gene ablation reduces nuclear ligand distribution and peroxisome proliferator activated receptor-α activity in cultured primary hepatocytes. *Arch. Biochem. Biophys. 485*, 160−173.
(29) Huang, H., McIntosh, A. L., Martin, G. G., Petrescu, A. D., Landrock, K., Landrock, D., Kier, A. B., and Schroeder, F. (2013) Inhibitors of fatty acid synthesis induced PPARα-regulated fatty acid b-oxidative enzymes: Synergistic roles of L-FABP and glucose. *PPAR Res.*, DOI: 10.1155/2013/865604.
(30) Petrescu, A. D., McIntosh, A. L., Storey, S. M., Huang, H., Martin, G. G., Landrock, D., Kier, A. B., and Schroeder, F. (2013) High glucose potentiates liver fatty acid binding protein (L-FABP) mediated fibrate induction of PPARα in mouse hepatocytes. *Biochim. Biophys. Acta 2013*, 1−22.
(31) Petrescu, A. D., Huang, H., Martin, G. G., McIntosh, A. L., Storey, S. M., Landrock, D., Kier, A. B., and Schroeder, F. (2012) Impact of L-FABP and glucose on polyunsaturated fatty acid induction of PPARα regulated b-oxidative enzymes. *Am. J. Physiol. 304*, G241−G256.
(32) Weisiger, R. A. (2005) Cytosolic fatty acid binding proteins catalyze two distinct steps in intracellular transport of their ligands. *Mol. Cell. Biochem. 239*, 35−42.
(33) McArthur, M. J., Atshaves, B. P., Frolov, A., Foxworth, W. D., Kier, A. B., and Schroeder, F. (1999) Cellular uptake and intracellular trafficking of long chain fatty acids. *J. Lipid Res. 40*, 1371−1383.
(34) Murphy, E. J. (1998) L-FABP and I-FABP expression increase NBD-stearate uptake and cytoplasmic diffusion in L-cells. *Am. J. Physiol. 275*, G244−G249.
(35) Atshaves, B. P., McIntosh, A. L., Lyuksyutova, O. I., Zipfel, W. R., Webb, W. W., and Schroeder, F. (2004) Liver fatty acid binding protein gene ablation inhibits branched-chain fatty acid metabolism in cultured primary hepatocytes. *J. Biol. Chem. 279*, 30954−30965.
(36) Paulussen, R. J. A., and Veerkamp, J. H. (1990) Intracellular fatty acid-binding proteins characteristics and function. In *Subcellular Biochemistry* (Hilderson, H. J., Ed.) pp 175−226, Plenum Press, New York.
(37) McIntosh, A. L., Huang, H., Atshaves, B. P., Wellburg, E., Kuklev, D. V., Smith, W. L., Kier, A. B., and Schroeder, F. (2010) Fluorescent n-3 and n-6 very long chain polyunsaturated fatty acids: Three photon imaging and metabolism in living cells overexpressing liver fatty acid binding protein. *J. Biol. Chem. 285*, 18693−18708.
(38) Long, D., and Yang, D. (2011) Millisecond timescale dynamics of human liver fatty acid binding protein: Testing of its relevance to the ligand entry process. *Biophys. J. 98*, 3054−3061.
(39) Long, D., and Yang, D. (2009) Buffer interference with protein dynamics: A case study on human liver fatty acid binding protein. *Biophys. J. 96*, 1482−1488.
(40) Carbone, V., and Velkov, T. (2013) Interaction of phthalates and phonxy acid herbicide environmental pollutants with intestinal intracellular lipid binding proteins. *Chem. Res. Toxicol. 26*, 1240−1250.
(41) Favretto, F., Assfalg, M., Gallo, M., Cicero, D. O., D'Onofrio, M., and Molinari, H. (2013) Ligand binding promiscuity and human liver fatty acid binding protein: Structural and dynamic insights from an interaction study with glycocholate and oleate. *ChemBioChem 14*, 1807−1819.
(42) Santambrogio, C., Favretto, F., D'Onofrio, M., Assfalg, M., Grandori, R., and Molinari, H. (2013) Mass spectrometry and NMR analysis of ligand binding by human liver fatty acid binding protein. *J. Mass Spectrom. 48*, 895−903.
(43) Robitaille, J., Brouillette, C., Lemieux, S., Perusse, L., Gaudet, D., and Vohl, M.-C. (2004) Plasma concentrations of apolipoprotein B are modulated by a gene-diet interaction effect between the L-FABP T94A polymorphism and dietary fat intake in French-Canadian men. *Mol. Genet. Metab. 82*, 296−303.
(44) Brouillette, C., Bose, Y., Perusse, L., Gaudet, D., and Vohl, M.-C. (2004) Effect of liver fatty acid binding protein (FABP) T94A missense mutation on plasma lipoprotein responsiveness to treatment with fenofibrate. *J. Hum. Genet. 49*, 424−432.
(45) Fisher, E., Weikert, C., Klapper, M., Lindner, I., Mohlig, M., Spranger, J., Boeing, H., Schrezenmeir, J., and Doring, F. (2007) L-FABP T94A is associated with fasting triglycerides and LDL-cholesterol in women. *Mol. Genet. Metab. 91*, 278−284.
(46) Weikert, M. O., Loeffelholz, C. v., Roden, M., Chandramouli, V., Brehm, A., Nowotny, P., Osterhoff, M. A., Isken, F., Spranger, J., Landau, B. R., Pfeiffer, A., and Mohlig, M. (2007) A Thr94Ala mutation in human liver fatty acid binding protein contributes to reduced hepatic glycogenolysis and blunted elevation of plasma glucsoe levels in lipid-exposed subjects. *Am. J. Physiol. 293*, E1078−E1084.
(47) Yamada, Y., Kato, K., Oguri, M., Yoshida, T., Yokoi, K., Watanabe, S., Metoki, N., Yoshida, H., Satoh, K., Ichihara, S., Aoyagi, Y., Yasunaga, A., Park, H., Tanaka, M., and Nozawa, Y. (2008) Association of genetic variants with atherothrombotic cerebral infarction in Japanese individuals with metabolic syndrome. *Int. J. Mol. Med. 21*, 801−808.
(48) Bu, L., Salto, L. M., De Leon, K. J., and De Leon, M. (2011) Polymorphisms in fatty acid binding protein 5 show association with type 2 diabetes. *Diabetes Res. Clin. Pract. 92*, 82−91.
(49) Peng, X.-E., Wu, Y. L., Lu, Q.-Q., Ju, Z.-J., and Lin, X. (2012) Two genetic variants in FABP1 and susceptibility to non-alcoholic fatty liver disease in a Chinese population. *Gene 500*, 54−58.
(50) Mansego, M. L., Martinez, F., Martinez-Larrad, M. T., Zabena, C., Rojo, G., Morcillo, S., Soriguer, F., Martin-Escudero, J. C., Serrano-Rios, M., Redon, J., and Chaves, F. J. (2012) Common variants of the liver fatty acid binding protein gene influence the risk of Type 2 diabetes and insulin resistance in Spanish population. *PLoS One 7*, e31853.
(51) Jackevicius, C. A., Tu, J. V., Ross, J. S., Ko, D. T., Carreon, D., and Krumholz, H. M. (2012) Use of fibrates in the United States and Canada. *JAMA, J. Am. Med. Assoc. 305*, 1217−1224.
(52) Lowe, J. B., Boguski, M. S., Sweetser, D. A., Elshourbagy, N., Taylor, J. M., and Gordon, J. I. (1985) Human liver fatty acid binding protein: Isolation of a full length cDNA and comparative sequence analyses of orthologous and paralogous proteins. *J. Biol. Chem. 260*, 3417.
(53) Chan, L., Wei, C. F., Li, W. H., Yang, C. Y., Ratner, P., Pownall, H., Gotto, A. M., Jr., and Smith, L. C. (1985) Human liver fatty acid binding protein cDNA and amino acid sequence. Functional and evolutionary implications. *J. Biol. Chem. 260*, 2629−2632.
(54) Maatman, R. G., van de Westerlo, E. M., Van Kuppevelt, T. H., and Veerkamp, J. H. (1992) Molecular identification of the liver- and the heart-type fatty acid-binding proteins in human and rat kidney. Use of the reverse transcriptase polymerase chain reaction. *Biochem. J. 288*, 285−290.
(55) Maatman, R. G., Degano, M., van Moerkerk, H. T., Van Marrewijk, W. J., Van der Horst, D. J., Sacchettini, J. C., and Veerkamp, J. H. (1994) Primary structure and binding characteristics of locust and human muscle fatty-acid-binding proteins. *Eur. J. Biochem. 221*, 801−810.
(56) Gao, N., Qu, X., Yan, J., Huang, Q., Yuan, H. Y., and Ouyang, D.-S. (2010) L-FABP T94A decreased fatty acid uptake and altered hepatic triglyceride and cholesterol accumulation in Chang liver cells stably transfected with L-FABP. *Mol. Cell. Biochem. 345*, 207−214.
(57) Chao, H., Zhou, M., McIntosh, A., Schroeder, F., and Kier, A. B. (2003) Acyl CoA binding protein and cholesterol differentially alter fatty acyl CoA utilization by microsomal acyl CoA:cholesterol transferase. *J. Lipid Res. 44*, 72−83.
(58) Smathers, R. L., Galligan, J. J., Shearn, C. T., Fritz, K. S., Mercer, K., Ronis, M., Orlicky, D. J., Davidson, N. O., and Petersen, D. R. (2013) Susceptibility of L-FABP −/− mice to oxidative stress in early-stage alcoholic liver. *J. Lipid Res. 54*, 1335−1345.
(59) Richert, L., Lamboley, C., Viollon-Abadie, C., Grass, P., Hartmann, N., Laurent, S., Heyd, B., Mantion, G., Chibout, S.-D., and Staedtler, F. (2003) Effects of clofibric acid on mRNA expression profiles in primary cultures of rat, mouse, and human hepatocytes. *Toxicol. Appl. Pharmacol. 191*, 130−146.

(60) Rakhshandehroo, M., Hooiveld, G., Muller, M., and Kersten, S. (2009) Comparative analysis of gene regulation by the transcription factor PPARα between mouse and human. *PLoS One 4*, e6796.
(61) Ito, Y., Nakamura, T., Yanagiba, Y., Ramdhan, D. H., Yamagishi, N., Naito, H., Kamijima, M., Gonzalez, F. J., and Nakajima, T. (2012) Plasticizers may activate human hepatic peroxisome proliferator activated receptor α less than that of a mouse but may activate constitutive androstane receptor in liver. *PPAR Res.*, DOI: 10.1155/2012/201284.
(62) Thompson, J., Winter, N., Terwey, D., Bratt, J., and Banaszak, L. (1997) The crystal structure of the liver fatty acid-binding protein. *J. Biol. Chem. 272*, 7140−7150.
(63) Betts, M. J., and Russell, R. B. (2003) Amino Acid Properties and Conseaquences of Substitutions. In *Bioinformatics for Geneticists* (Barnes, M. R., and Gray, I. C., Eds.) pp 289−316, Wiley, New York.
(64) Zomer, A. W. M., van der Burg, B., Jansen, G. A., Wanders, R. J. A., Poll-The, B. T., and van der Saag, P. T. (2000) Pristanic acid and phytanic acid: Naturally occurring ligands for the nuclear receptor peroxisome proliferator activated receptor α. *J. Lipid Res. 41*, 1801−1807.
(65) Wolfrum, C., and Spener, F. (2000) Fatty acids as regulators in lipid metabolism. *Eur. J. Lipid Sci. Technol. 102*, 746−762.
(66) Chapman, M. J. (2003) Fibrates in 2003: Therapeutic action in atherogenic dyslipidemia and future perspectives. *Atherosclerosis 171*, 1−13.
(67) Dayspring, T., and Pokrywka, G. (2006) Fibrate therapy in patients with metabolic syndrome and diabetes mellitus. *Curr. Atheroscler. Rep. 8*, 356−364.
(68) Desvergne, B., Michalik, L., and Wahli, W. (2004) Be fit or be sick: Peroxisome proliferator-activated receptors are down the road. *Mol. Endocrinol. 18*, 1321−1332.
(69) Staels, B., Maes, M., and Zambon, A. (2008) Fibrates and future PPARα agonists in the treatment of cardiovascular disease. *Nat. Clin. Pract. Cardiovasc. Med. 5*, 542−553.
(70) Winter, N. S., Gordon, J. I., and Banaszak, L. J. (1990) Characterization of crystalline rat liver fatty acid binding protein produced in *Escherichia coli*. *J. Biol. Chem. 265*, 10955−10958.
(71) Cai, J., Lucker, C., Chen, Z., Klimtchuk, E., Qiao, Y., and Hamilton, J. A. (2009) Human liver fatty acid binding protein: Solution structure and ligand binding. *Biophys. J. 96*, 600a.
(72) Cai, J., Lucke, C., Qiao, Y., Klimtchuk, E., and Hamilton, J. A. (2010) Solution structure and backbone dynamics of human liver fatty acid binding protein. *Biophys. J. 98*, 238a.
(73) Tanfani, F., Kochan, Z., Swierczynski, J., Zydowo, M. M., and Bertoli, E. (1995) Structural properties and thermal stability of human liver and heart fatty acid binding proteins: A Fourier transform IR spectroscopy study. *Biopolymers 36*, 569−577.
(74) Jolly, C. A., Hubbell, T., Behnke, W. D., and Schroeder, F. (1997) Fatty acid binding protein: Stimulation of microsomal phosphatidic acid formation. *Arch. Biochem. Biophys. 341*, 112−121.
(75) Jolly, C. A., Murphy, E. J., and Schroeder, F. (1998) Differential influence of rat liver fatty acid binding protein isoforms on phospholipid fatty acid composition: Phosphatidic acid biosynthesis and phospholipid fatty acid remodeling. *Biochim. Biophys. Acta 1390*, 258−268.
(76) Schroeder, F., Jolly, C. A., Cho, T. H., and Frolov, A. A. (1998) Fatty acid binding protein isoforms: Structure and function. *Chem. Phys. Lipids 92*, 1−25.
(77) Hostetler, H. A., Lupas, D., Tan, Y., Dai, J., Kelzer, M. S., Martin, G. G., Woldegiorgis, G., Kier, A. B., and Schroeder, F. (2011) Acyl-CoA binding proteins interact with the acyl-CoA binding domain of mitochondrial carnitine palmitoyltransferase I. *Mol. Cell. Biochem. 355*, 135−148.
(78) Storey, S. M., McIntosh, A. L., Huang, H., Martin, G. G., Landrock, K. K., Landrock, D., Payne, H. R., Kier, A. B., and Schroeder, F. (2012) Loss of intracellular lipid binding proteins differentially impacts saturated fatty acid uptake and nuclear targeting in mouse hepatocytes. *Am. J. Physiol. 303*, G837−G850.
(79) Atshaves, B. P., Storey, S. M., Petrescu, A. D., Greenberg, C. C., Lyuksyutova, O. I., Smith, R., and Schroeder, F. (2002) Expression of fatty acid binding proteins inhibits lipid accumulation and alters toxicity in L-cell fibroblasts. *Am. J. Physiol. 283*, C688−C703.
(80) Martin, G. G., Danneberg, H., Kumar, L. S., Atshaves, B. P., Erol, E., Bader, M., Schroeder, F., and Binas, B. (2003) Decreased liver fatty acid binding capacity and altered liver lipid distribution in mice lacking the liver fatty acid binding protein (L-FABP) gene. *J. Biol. Chem. 278*, 21429−21438.
(81) Wolfrum, C., Buhlman, C., Rolf, B., Borchers, T., and Spener, F. (1999) Variation of liver fatty acid binding protein content in the human hepatoma cell line HepG2 by peroxisome proliferators and antisense RNA affects the rate of fatty acid uptake. *Biochim. Biophys. Acta 1437*, 194−201.
(82) Oosterveer, M. H., Grefhourst, A., van Dijk, T. H., Havinga, R., Staels, B., Kuipers, F., Groen, A. K., and Reijngoud, D.-J. (2009) Fenofibrate simultaneously induces hepatic fatty acid oxidation, synthesis, and elongation in mice. *J. Biol. Chem. 284*, 34036−34044.
(83) Sekiya, M., Yhagi, N., Matsuzaka, T., Najima, Y., Nakakuki, M., Nagai, R., Ishibashi, S., Osuga, J.-I., Yamada, N., and Shimano, H. (2003) Polyunsaturated fatty acids ameliorate hepatic steatosis in obese mice by SREBP-1 suppression. *Hepatology 38*, 1529−1539.
(84) Froyland, L., Madsen, L., Vaagenes, H., Totland, G. K., Auwerx, J., Kryvi, H., Staels, B., and Berge, R. K. (1997) Mitochondrion is the principal target for nutritional and pharmacological control of triglyceride metabolism. *J. Lipid Res. 38*, 1851−1858.
(85) Bijland, S., Pieterman, E. J., Maas, A. C. E., van der Hoorn, J. W. A., van Erk, M. J., van Klinken, J. B., Havekes, L. M., van Dijk, K. W., Princen, H. M., and Rensen, P. C. N. (2010) Fenofibrate increases VLDL triglyceride production despite reducing plasma triglyceride levels in APOE3-Leiden.CETP mice. *J. Biol. Chem. 285*, 25168−25175.
(86) Robins, S. J. (2002) Fibrates and coronary heart disease reduction. *Curr. Opin. Endocrinol. Diabetes 9*, 312−322.
(87) Saha, S. A., and Arora, R. R. (2010) Fibrates in the prevention of cardiovascular disease in pateints with type 2 diabetes mellitus: A pooled meta-analysis of randomized placebo-controlled clinical trials. *Int. J. Cardiol. 141*, 157−166.
(88) Frederiksen, K. S., Wulf, E. M., Wassermann, K., Sauerberg, P., and Fleckner, J. (2003) Identification of hepatic transcriptional changes in insulin-resistant rats treated with peroxisome proliferator activated receptor-α agonists. *J. Mol. Endocrinol. 30*, 317−329.
(89) Otvos, J. D., Collins, D., Freedman, D. S., Shaluarova, I., Schaefer, E. J., McNamara, J. R., Bloomfield, H. E., and Robins, S. J. (2006) Low-density lipoprotein and high-density lipoproteion particle subclasses predict coronary events and are favorably changed by gemfibrozil therapy in the Veterans Affairs high density lipoprotein intervention trial. *Circulation 113*, 1556−1563.
(90) Heinaniemi, M., Uski, J. O., Degenhart, T., and Carlberg, C. (2007) Meta-analysis of primary target genes of peroxisome proliferator-activated receptors. *Genome Biol. 8*, R147.
(91) Rakhshandehroo, M., Knoch, B., Muller, M., and Kersten, S. (2010) Peroxisome proliferator-activated receptor α target genes. *PPAR Res.*, DOI: 10.1155/2010/612089.
(92) Atshaves, B. P., Payne, H. R., McIntosh, A. L., Tichy, S. E., Russell, D., Kier, A. B., and Schroeder, F. (2004) Sexually dimorphic metabolism of branched chain lipids in C57BL/6J mice. *J. Lipid Res. 45*, 812−830.